AD-A155 188 RHODIUM-103 AND INDIUM-115 INELASTIC SCATTERING REACTIONS FOR FISSION NEUTRON DOSIMETRY(U) ARMED FORCES RADIOBIOLOGY RESEARCH INST BETHESDA MD G H ZEMAN 1/1

UNCLASSIFIED DEC 84 AFRRI-TR84-7 F/G 20/8 NL

END

FILMED

DTIC

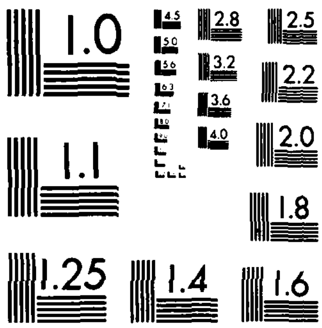

MICROCOPY RESOLUTION TEST CHART
NATIONAL BUREAU OF STANDARDS-1963-A

2

AFRRI TECHNICAL REPORT

Rhodium-103 and indium-115 inelastic scattering reactions for fission neutron dosimetry

G. H. Zeman

AFRRI TR84-7

DEFENSE NUCLEAR AGENCY
ARMED FORCES RADIOBIOLOGY RESEARCH INSTITUTE
BETHESDA, MARYLAND 20814-5145

APPROVED FOR PUBLIC RELEASE; DISTRIBUTION UNLIMITED

UNCLASSIFIED
SECURITY CLASSIFICATION OF THIS PAGE

A 155 188

REPORT DOCUMENTATION PAGE

1a. REPORT SECURITY CLASSIFICATION: UNCLASSIFIED	1b. RESTRICTIVE MARKINGS
2a. SECURITY CLASSIFICATION AUTHORITY	3. DISTRIBUTION/AVAILABILITY OF REPORT: Approved for public release; distribution unlimited.
2b. DECLASSIFICATION/DOWNGRADING SCHEDULE	
4. PERFORMING ORGANIZATION REPORT NUMBER(S): AFRRI-TR84-7	5. MONITORING ORGANIZATION REPORT NUMBER(S)
6a. NAME OF PERFORMING ORGANIZATION: Armed Forces Radiobiology Research Institute; 6b. OFFICE SYMBOL (If applicable): AFRRI	7a. NAME OF MONITORING ORGANIZATION
6c. ADDRESS (City, State and ZIP Code): Defense Nuclear Agency, Bethesda, Maryland 20814-5145	7b. ADDRESS (City, State and ZIP Code)
8a. NAME OF FUNDING/SPONSORING ORGANIZATION: Defense Nuclear Agency; 8b. OFFICE SYMBOL (If applicable): DNA	9. PROCUREMENT INSTRUMENT IDENTIFICATION NUMBER
8c. ADDRESS (City, State and ZIP Code): Washington, DC 20305	10. SOURCE OF FUNDING NOS.
11. TITLE (Include Security Classification): (See cover)	

PROGRAM ELEMENT NO.	PROJECT NO.	TASK NO.	WORK UNIT NO.
NWED QAXM			MJ 00137

12. PERSONAL AUTHOR(S): Zeman, G. H.

13a. TYPE OF REPORT	13b. TIME COVERED	14. DATE OF REPORT (Yr., Mo., Day)	15. PAGE COUNT
Technical	FROM ____ TO ____	December 1984	21

16. SUPPLEMENTARY NOTATION

17. COSATI CODES			18. SUBJECT TERMS (Continue on reverse if necessary and identify by block number)
FIELD	GROUP	SUB. GR.	

19. ABSTRACT (Continue on reverse if necessary and identify by block number)

Neutron activation foil cross sections are calculated for shielded and unshielded configurations of the AFRRI TRIGA reactor. The neutron spectra used in the calculations ranged in average energy from 0.55 MeV to 3.4 MeV, and the total range of activation foil sensitivity factors (cross section per unit tissue-kerma) was ±8.5% for ^{103}Rh (n,n') ^{103m}Rh, ±20% for ^{115}In (n,n') ^{115m}In, and ±75% for ^{32}S (n,p)^{32}P. These results support the use of ^{103}Rh and ^{115}In activation foils as tissue-kerma dosimeters at the AFRRI TRIGA reactor.

20. DISTRIBUTION/AVAILABILITY OF ABSTRACT: UNCLASSIFIED/UNLIMITED ☐ SAME AS RPT. ☒ DTIC USERS ☐	21. ABSTRACT SECURITY CLASSIFICATION: UNCLASSIFIED	
22a. NAME OF RESPONSIBLE INDIVIDUAL: J. A. Van Deusen	22b. TELEPHONE NUMBER (Include Area Code): (202) 295-3536	22c. OFFICE SYMBOL: ADMG

DD FORM 1473, 83 APR EDITION OF 1 JAN 73 IS OBSOLETE

UNCLASSIFIED
SECURITY CLASSIFICATION OF THIS PAGE

CONTENTS

Introduction	3
Theory	4
Methods	8
Results	11
Discussion	14
References	16

INTRODUCTION

Using activation foils to measure neutron kerma requires knowledge of the neutron energy spectrum. This knowledge can be gained either through analyzing the responses of different threshold activation foils or by radiation transport calculations. During the last few years, neutron energy spectra of the AFRRI TRIGA* reactor (1) have been examined in three calculational efforts (2-4) and two experimental efforts (5-6). These studies defined TRIGA neutron energy spectra (a) free in air and (b) within experimental arrays and phantoms for lead, water, or no shielding between the reactor core and the points of measurement. As a result, it is now possible to predict with high confidence the responses of neutron activation foils under a variety of conditions of experimental irradiation.

In this report the average cross sections for inelastic neutron scattering reactions in ^{103}Rh and ^{115}In are derived. These detectors show potential for direct measurement of neutron kerma in the TRIGA reactor experimental arrays for which spectral information is available. Experimental procedures for use of ^{103}Rh and ^{115}In and intercomparison with other dosimetry techniques are not covered here, but will be reported separately.

---

* Training, Research, and Isotope Production
General Atomic

THEORY

Inelastic neutron scattering reactions in ^{103}Rh and ^{115}In are described in Table 1. The potential use of ^{103}Rh for the dosimetry of fission neutrons, first recognized by Ing and Cross (8) over 10 years ago, is based on the close correspondence between the cross section of ^{103}Rh and the kerma response of muscle for neutrons in the energy range of 0.7 to 7 MeV (Figure 1). In this respect, ^{115}In appears less well suited for fission neutron dosimetry, but in many situations the longer half-life of its activation product may make it preferable to ^{103}Rh.

Table 1. Physical Data for Inelastic Neutron Scattering in ^{103}Rh and ^{115}In

	Reaction	
	^{103}Rh (n,n') ^{103m}Rh	^{115}In (n,n') ^{115m}In
Target isotopic abundance	1.00	0.96
Effective threshold	0.7 MeV	1.4 MeV
Product half-life (ref. 7)	56.1 min	4.50 hr
Product radiations (ref. 7):		
Gamma	39.7 keV (0.06%)	335.6 keV (39.25%) 497.3 (0.05%)
X-ray	20.2 (4.36%) 20.0 (2.19%) 22.7 (1.07%)	24.2 (20.30%) 24.0 (10.32%) 27.2 (5.29%) 27.9 (1.06%)

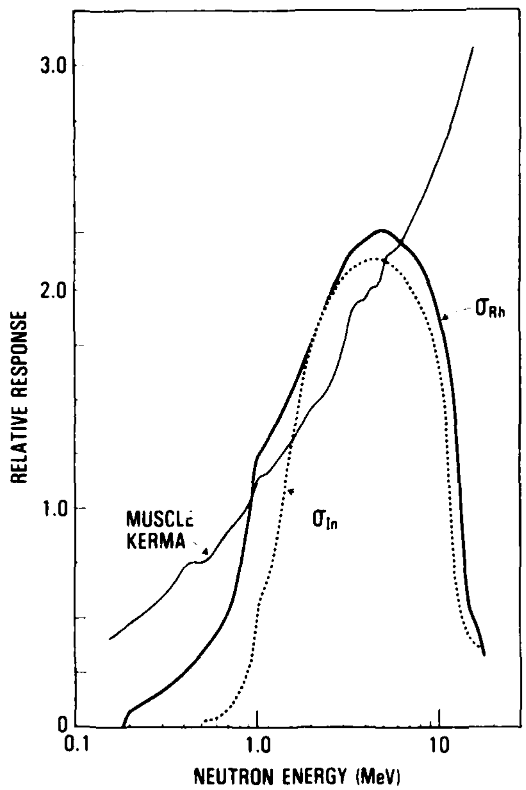

Figure 1. Neutron kerma in muscle and reaction cross sections for $^{103}Rh\ (n,n')^{103m}Rh$ and $^{115}In\ (n,n')^{115m}In$. Linear scales were normalized to display relative shapes of curves.

Figure 2 shows neutron kerma spectra for cases that constitute the extremes of spectral variation encountered in radiobiology experiments with the AFRRI TRIGA reactor. The fluence-averaged energies of these spectra range from 0.5 MeV (within the phantom behind a 15-cm lead shield) to 3.4 MeV (free-in-air behind a 30-cm water shield) (9). Except for the 30-cm water shield, less than 3% of the neutron kerma from TRIGA spectra arises from neutrons with energies over 7 MeV, so the high-energy falloff in ^{103}Rh and ^{115}In cross sections poses no obstacle to dosimetric applications. However, a large fraction of the neutron kerma is due to neutrons with energies below 1 MeV, for which both the ^{103}Rh and the ^{115}In cross sections are rapidly falling. This low-energy falloff places fundamental limits on the dosimetric accuracy that may be attained with either detector.

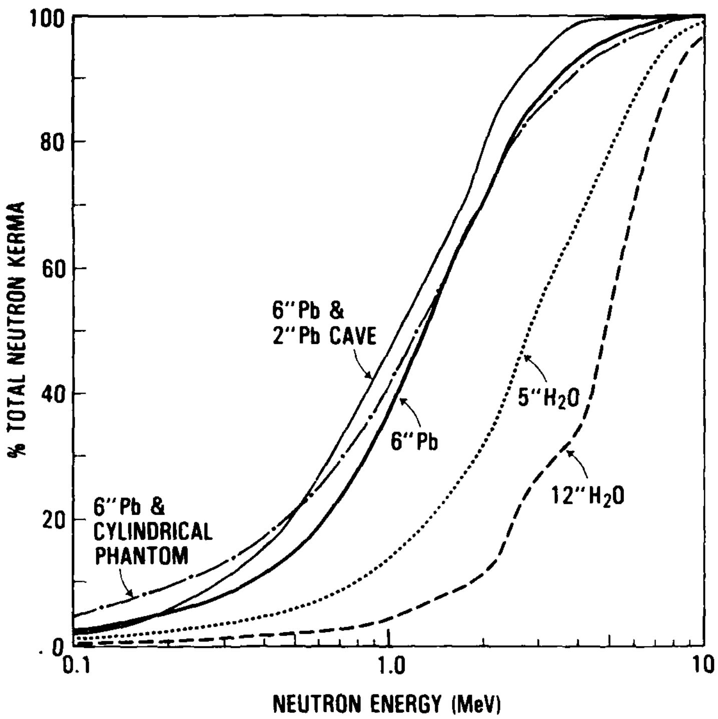

Figure 2. Cumulative neutron kerma spectra for selected TRIGA reactor arrays. Ordinates give fraction of total neutron kerma due to neutrons with energies less than or equal to values on abscissa. Thermal neutron kerma was excluded (see Table 2). Curves were obtained from group spectra by cubic splines interpolation between integral group kerma values.

The degree to which either ^{103}Rh or ^{115}In may be useful for absolute neutron dosimetry can be assessed by computing the spectrum-averaged cross section, $\bar{\sigma}$, and spectrum-averaged kerma factor, $\bar{K}$, for each neutron spectrum. These quantities are defined below.

$$\bar{\sigma} = \frac{\int_{0.4\,eV}^{\infty} \sigma(E)\phi(E)dE}{\int_{0.4\,eV}^{\infty} \phi(E)dE} = \frac{\sum_{g=1}^{36} \sigma_g \phi_g \Delta E_g}{\sum_{g=1}^{36} \phi_g \Delta E_g}$$

$$\bar{K} = \frac{\int_{0.4\,eV}^{\infty} K(E)\phi(E)dE}{\int_{0.4\,eV}^{\infty} \phi(E)dE} = \frac{\sum_{g=1}^{36} K_g \phi_g \Delta E_g}{\sum_{g=1}^{36} \phi_g \Delta E_g}$$

In the above, $\phi(E)$ and ϕg represent the neutron energy spectrum, E the neutron energy, $\sigma(E)$ and σg the reaction cross section, and K(E) and Kg the neutron kerma. The integrals exclude thermal neutrons since these constitute only a small fraction of the total kerma (see Table 2), and can be adequately measured by other techniques, such as the cadmium difference method. The sums extend over all energy groups, g (except thermal, group 37), of the Oak Ridge Data Library Collection 31 (DLC-31) (10) format in which TRIGA neutron spectra have been compiled.

Table 2. Kerma Due to Thermal Neutrons

Shield/Array*	Thermal Neutron Kerma (% Total Neutron Kerma)
6" Pb/cylindrical phantom	6.2
2" Pb/monkey phantom head, trunk	2.8, 3.8
2" Pb/exercise wheel	0.6
None/free-in air ER 2†	0.5

*See references 2 and 4 for shield/array descriptions.
†Exposure Room 2

Spectrum-averaged cross sections, $\bar{\sigma}$, are expressed in units of barns (10^{-24} cm^2) or, more simply, activation per atom per unit fluence. Spectrum-averaged kerma factors, $\bar{K}$, are in units gray per unit fluence. Consequently, the ratio $\bar{\sigma}/\bar{K}$ has units activation per atom per gray, and represents a detector's sensitivity or calibration factor for kerma measurements in a neutron spectrum. In what follows, the quantities $\bar{\sigma}$ and $\bar{K}$ are computed for several TRIGA neutron spectra, and the ratios $\bar{\sigma}/\bar{K}$ are analyzed as sensitivity factors for neutron kerma measurements with ^{103}Rh and ^{115}In. For comparison, ratios $\bar{\sigma}/\bar{K}$ for sulfur activation via ^{32}S (n,p) ^{32}P are also presented.

METHODS

Neutron kerma factors for muscle from ICRU Report 26 (11) were regrouped to the DLC-31 format as previously described (12). Cross sections for inelastic neutron scattering in ^{103}Rh and ^{115}In from ICRU Report 26 were group averaged (σ versus log E) to the DLC-31 format using cubic-splines interpolation. Cross sections for sulfur activation were taken from reference 5. All cross sections are shown in Table 3. All results are presented using the following units:

$\bar{K}$: 10^{-12} gray per neutron per cm^2

$\bar{\sigma}/\bar{K}$: 10^{-21} activations per atom per gray

Table 3. Group Cross Sections (Barns)

Group Upper Energy (MeV)	$^{103}Rh\ (n,n')\ ^{103m}Rh$	$^{115}In\ (n,n')\ ^{115m}In$	$^{32}S\ (n,p)\ ^{32}P$
19.6	0.162	0.056	0.112
16.9	0.223	0.057	0.171
14.9	0.265	0.061	0.225
14.2	0.310	0.066	0.253
13.8	0.418	0.083	0.291
12.8	0.588	0.113	0.331
12.2	0.729	0.160	0.376
11.1	0.838	0.222	0.380
10.0	0.916	0.263	0.355
9.0	0.973	0.279	0.333
8.2	1.007	0.289	0.323
7.4	1.041	0.302	0.316
6.4	1.072	0.314	0.273
5.0	1.091	0.320	0.237
4.7	1.088	0.321	0.300
4.1	1.057	0.316	0.198
3.0	0.972	0.302	0.091
2.4	0.915	0.288	0.0896
2.3	0.858	0.265	0.0362
1.8	0.715	0.158	0.00103
1.1	0.366	0.033	0
0.55	0.082	0.001	
0.16	0	0	

Thirty-five neutron spectra from three separate sources (2-4) were used in this analysis. Descriptions of the TRIGA reactor configurations to which the spectra apply are given in the references cited in Tables 4a and 4b. The primate restraint chair and physical activity wheel arrays are further described in reference 13. Each spectrum represents the total (integrated 4-pi) neutron fluence at the specified measurement point. All spectra were originally compiled in the DLC-31 format and were used in that format for the present calculations.

Table 4a. Kerma and Cross Sections for Unshielded TRIGA Arrays

Array	Ref. No.	Distance to Core Center (cm)	$\bar{K}$	$\bar{\sigma}_{Rh}/\bar{K}$	$\bar{\sigma}_{In}/\bar{K}$	$\bar{\sigma}_{S}/\bar{K}$
Free in air, ER 1	3	30	17.2	2252	576	237
	2	50	19.9	2284	594	256
	2	100	20.5	2341	620	252
	2	200	18.1	2270	589	252
	2	300	16.2	2248	579	243
	2	400	14.4	2217	566	231
	2	500	12.9	2192	556	224
Free in air, ER 2	3	30	16.8	2258	578	234
	2	50	18.1	2291	599	261
	2	100	18.5	2343	613	238
	2	200	15.4	2256	584	248
	2	300	13.3	2218	577	233
Physical activity wheel, ER 1, without phantom	3	150	12.1	2186	553	187
Primate restraint chair, ER 1, without phantom	3	85	17.1	2271	586	248
	3	100	16.9	2268	585	247
	3	150	16.1	2257	580	242
Primate restraint chair, ER 2:						
Without phantom	3	125	16.1	2256	580	242
Without phantom	3	200	14.2	2230	569	232
Monkey midhead	4	100	13.7	2207	561	237
Monkey midtrunk	4	100	13.7	2217	559	237

Table 4b. Kerma and Cross Sections for Shielded TRIGA Arrays

Array	Ref. No.	Distance to Core Center (cm)	$\overline{K}$	$\bar{\sigma}_{Rh}/\overline{K}$	$\bar{\sigma}_{In}/\overline{K}$	$\bar{\sigma}_{S}/\overline{K}$
2" Pb Shield, ER 1						
Free in air	2	100	20.5	2283	568	202
Physical activity wheel:						
Without phantom	2	90	16.4	2179	533	187
Without phantom	3	90	11.5	2094	498	168
Primate restraint chair:						
Without phantom	3	90	15.6	2175	525	181
Monkey midhead	4	100	11.8	2113	511	188
Monkey trunk	4	100	11.8	2140	519	193
6" Pb Shield, ER 1						
Free in air	2	100	17.2	2071	455	111
Cylindrical phantom	2	100	9.91	1956	435	120
2" Pb cave	2	100	13.7	1940	404	68
Primate restraint chair without phantom	3	100	13.8	1997	424	100
5" H_2O Shield, ER 1						
Free in air	3	42.5	21.7	2320	619	300
Free in air	2	100	23.9	2347	637	320
Primate restraint chair without phantom	3	100	21.8	2336	631	318
12" H_2O Shield, ER 1						
Free in air	2	100	34.5	2321	663	477

RESULTS

Calculated values of $\overline{K}$ and $\bar{\sigma}/\overline{K}$ for the neutron spectra are presented in Table 4. For ^{103}Rh, the highest value (7.5 cm H_2O shield) and lowest value (15 cm Pb with cave) of $\bar{\sigma}/\overline{K}$ were found to differ by 17%. This difference corresponds closely to that in the fraction of total neutron kerma due to energies below 0.6 MeV (see Figure 2). For ^{115}In, the highest value (30 cm H_2O shield) and lowest value (15 cm Pb with cave) of $\bar{\sigma}/\overline{K}$ differed by almost 40%, which reflects the fraction of total kerma due to neutrons with energy below about 1.5 MeV. Thus the calculations tend to support the intuitive interpretations ascribed to Figures 1 and 2.

In Table 5, the activation foil kerma sensitivities, $\bar{\sigma}/\bar{K}$, are summarized by the type of reactor shield. This summary shows explicitly the reduced spectral variability of ^{103}Rh compared to ^{115}In and ^{32}S for kerma measurements. When ^{103}Rh sensitivities, grouped by shield, are separated into either free-in-air or phantom/array measurements, variations in $\bar{\sigma}/\bar{K}$ are reduced to below ± 4% (two sigma). This indicates strong potential for use of ^{103}Rh in absolute neutron kerma and depth distribution measurements in experimental arrays and phantoms.

Table 5. Summary of Activation Foil Kerma Sensitivities*

Reactor Shield	All Spectra	Free-in-Air Spectra	Array/Phantom Spectra
		$\bar{\sigma}_{Rh}$ $\bar{K}$ ± SD (N)	
6" Pb	1991 ± 2.9% (4)	2071 (1)	1964 ± 1.5% (3)
2" Pb	2164 ± 3.1% (6)	2283 (1)	2152 ± 1.5% (5)
None (30-200 cm)	2662 ± 1.9% (16)	2287 ± 1.6% (8)	2237 ± 1.4% (8)
5" or 12" H_2O	2331 ± 0.6% (4)	2329 ± 0.7% (3)	2336 (1)
		$\bar{\sigma}_{In}$ $\bar{K}$ ± SD (N)	
6" Pb	430 ± 5.0% (4)	455 (1)	421 ± 3.7% (3)
2" Pb	526 ± 4.6% (6)	568 (1)	517 ± 2.6% (5)
None (30-200 cm)	583 ± 3.1% (16)	594 ± 2.7% (8)	572 ± 2.2% (8)
5" or 12" H_2O	638 ± 2.9% (4)	640 ± 3.4% (3)	631 (1)
		$\bar{\sigma}_{S}$ $\bar{K}$ ± SD (N)	
6" Pb	100 ± 23% (4)	111 (1)	96 ± 27% (3)
2" Pb	187 ± 6.2% (6)	202 (1)	183 ± 5.2% (5)
None (30-200 cm)	241 ± 6.9% (16)	247 ± 4.0% (8)	234 ± 8.4% (8)
5" or 12" H_2O	354 ± 23% (4)	365 ± 27% (3)	318 (1)

*Entries are in units 10^{-21} activations per atom per gray.

The present work for TRIGA neutron spectra can be compared to published information for other fission neutron spectra, notably the compendium of spectra published by the International Atomic Energy Agency (IAEA) (14). This comparison is shown in Figure 3.

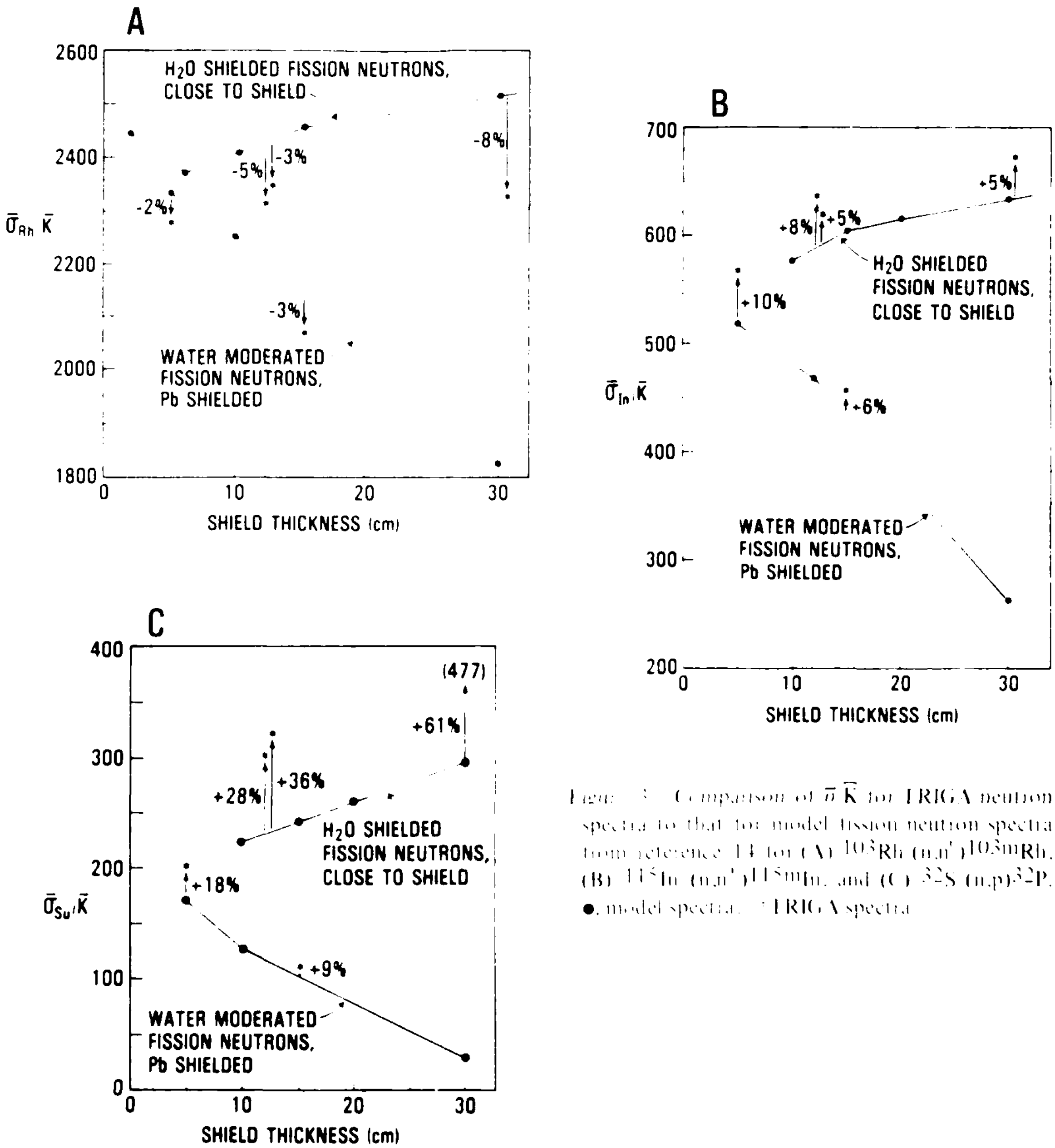

Figure 3. Comparison of $\bar{\sigma}\bar{K}$ for TRIGA neutron spectra to that for model fission neutron spectra from reference 14 for (A) $^{103}Rh(n,n')^{103m}Rh$, (B) $^{115}In(n,n')^{115m}In$, and (C) $^{32}S(n,p)^{32}P$. ●, model spectra; TRIGA spectra

Relative to IAEA neutron spectra and calculations, the present work gives values of $\bar{\sigma}/\bar{K}$ 2%-8% lower than expected for ^{103}Rh, 5%-10% higher than expected for ^{115}In, and considerably larger variations for ^{32}S. Reasons for these deviations have not been positively identified, but probably include the fact that the model spectra of IAEA do not represent adequately the TRIGA reactor core, pool, tank wall, or exposure rooms. However, it is difficult to imagine how spectral differences could cause overestimation of $\bar{\sigma}/\bar{K}$ for one detector and underestimation for another. Thus it seems likely that differences must also exist between the cross section and kerma values used by IAEA and those used here, either in basic physical data or in the formatting of that data into spectrum energy groups.

DISCUSSION

The calculations of ^{103}Rh and ^{115}In *inelastic scattering* cross sections presented in this report establish the feasibility of using these reactions for directly measuring neutron kerma in TRIGA reactor neutron spectra. The neutron spectra included in this analysis ranged in average energy from 0.55 to 3.4 MeV, and the total range of activation foil sensitivity factors (activation per atom per gray) was ± 8.5% for ^{103}Rh, ± 20% for ^{115}In, and + 75% for S. By grouping the sensitivity factors according to (a) reactor shield and (b) irradiation condition either free in air or in presence of a phantom/array, it was found that group sensitivity factors with high precision (± 4% two sigma) applied to the use of ^{103}Rh, and with lower precision (± 8% two sigma) to ^{115}In. These findings suggest that ^{103}Rh may have potential for the more accurate measurement of fission neutron kerma than the 5%-10% uncertainty associated with ionization chamber techniques (15).

Uncertainties in the neutron energy spectra used in this analysis, as well as in the cross sections and kerma factors, place limitations on the accuracy that can be ascribed to the resulting foil sensitivity factors. An additional accuracy-limiting factor is the representation of spectra, cross sections, and kerma in energy groups of rather broad width (0.11-0.55, 0.55-1.1, and 1.1-1.8 MeV) near the detector threshold energies. It is clear that uncertainties in muscle kerma factors or cross sections would have a spectrum-weighted proportionate effect on the calculated foil sensitivity factors. It is less clear what impact results from spectral uncertainties or finite group widths, especially in light of the relative invariance of the foil sensitivity factors over the range of spectra studied. In this regard, comparison of selected $\bar{\sigma}/\bar{K}$ values derived in the present work with appropriate values from the IAEA spectrum compendium (14) revealed differences ranging from -2% to -8% for ^{103}Rh, from +5% to +10% for ^{115}In, and from +9% to +61% for ^{32}S. The negative differences for ^{103}Rh suggest a low-energy neutron kerma component in the TRIGA exposure rooms, but the positive differences for ^{115}In and ^{32}S remain unexplained. Those differences may be resolvable through experimental intercomparison in TRIGA neutron fields of ^{103}Rh, ^{115}In, and ^{32}S activation foils together with paired ionization chamber or calorimetric techniques.

Aside from absolute accuracy considerations, the present results indicate that, for a given reactor shield, the changes in ^{103}Rh and ^{115}In foil sensitivities are small between different array types, either free in air or at midline in a phantom. From this can be concluded that these foils, especially ^{103}Rh, can be used to advantage for defining the relative neutron kerma distribution within an array or at different depths in animal phantoms.

ACKNOWLEDGMENT

The author thanks Mr. D. Eagleson for assistance in some of the calculations presented in this report.

REFERENCES

1. Sholtis, J. A., Jr., and Moore, M. L. Reactor facility at Armed Forces Radiobiology Research Institute. Technical Report TR81-2, Armed Forces Radiobiology Research Institute, Bethesda, Maryland, 1981.
2. Verbinski, V. V., and Cassapakis, C. G. Calculation of the neutron and gamma-ray environment in and around the TRIGA reactor, Volume II. DNA Report No. 5793F-2. Defense Nuclear Agency, Washington, DC, June 1981.
3. Johnson, J. O., et al. Calculation of radiation fields and monkey mid-head and mid-thorax responses in AFRRI-TRIGA reactor facility experiments. ORNL Technical Manual TM-8807, Oak Ridge National Laboratory, Oak Ridge, Tennessee, July 1983.
4. Kaul, D. C., et al. Phantom dosimetry calculations for use in radiation effects correlations. Final

Report, Contract DNA 001-83-C-0187. Defense Nuclear Agency, Washington, DC, 30 July 1984.

5. Verbinski, V. V., Cassapakis, C. C., Hagan, W. K., Ferlic, K., and Daxon, E. Radiation field characterization for the AFFRI TRIGA reactor. Volume 1, Baseline data and evaluation of calculational data. DNA Report No. 5793F-1, Defense Nuclear Agency, Washington, DC, June 1981.

6. Verbinski, V. V., et al. Neutron spectrum in monkey phantom. Ongoing Defense Nuclear Agency contract, March 1984.

7. Medical Internal Radiation Dose Committee. Radionuclide decay schemes and nuclear parameters for use in radiation dose estimation. MIRD Pamphlet No. 10, Society of Nuclear Medicine, New York, 1975.

8. Ing, H., and Cross, W. G. A criticality neutron dosimeter using the ^{103}Rh (n,n') ^{103m}Rh reaction. Health Physics 25: 291-297, 1975.

9. Ferlic, K. P. and Zeman, G. H. Spectrum averaged kerma factors for reactor dosimetry with paired ion chambers. Technical Report TR83-2, Armed Forces Radiobiology Research Institute, Bethesda, Maryland, 1983.

10. Bartine, D. E., et al. Production and testing of the DNA few-group coupled neutron-gamma cross-section library. ORNL Technical Manual TM-4840, Oak Ridge National Laboratory, Oak Ridge, Tennessee, March 1977.

11. Neutron dosimetry for biology and medicine. Report No. 26, International Commission on Radiation Units and Measurements, Washington, DC, January 1977.

12. Zeman, G. H. and Bice, W. S., Jr. Kerma factors for use in 37-group neutron spectrum calculations. Technical Report TR83-3, Armed Forces Radiobiology Research Institute, Bethesda, Maryland, 1983.

13. Franz, C. G., Young, R. W., and Mitchell, W. E. Behavioral studies following ionizing radiation exposures: A data base. Technical Report TR81-4, Armed Forces Radiobiology Research Institute, Bethesda, Maryland, 1981.

14. Ing, H. and Makra, S. Compendium of neutron spectra in criticality accident dosimetry. IAEA Report 180, International Atomic Energy Agency, Vienna, 1978.

15. Broerse, J. J., Mijnheer, B. J., and Williams, J. R. European protocol for neutron dosimetry for external beam therapy. British Journal of Radiology 54: 882-898, 1981.

END

FILMED

7-85

DTIC